

MEASURING LOSSES OF AN AIR-CORE SHUNT REACTOR WITH AN ADVANCED LOSS MEASURING SYSTEM

J. Havunen¹, E.-P. Suomalainen¹, J. Tornberg², J. Hällström¹, T. Lehtonen¹ and A. Merviö²

¹VTT Technical Research Centre of Finland Ltd, National Metrology Institute VTT MIKES, P.O. Box 1000, FI-02044 VTT, Finland

²GE Grid Solutions Ltd, P.O. Box 4, FI-33331, Tampere, Finland

*Email: jussi.havunen@vtt.fi

Abstract: Losses of low-loss inductive components like power transformers and reactors are difficult to measure accurately because of the very low power factor. Low power factor means that accuracy of the measurement of the phase angle is a crucial factor in the measurement uncertainty. In this paper we introduce an advanced loss measurement system for measuring the losses of an air-core reactor under high voltage. The system consists of a capacitive voltage divider, a current sensor and two sampling multimeters. The high-voltage arm of the used capacitive divider is a gas-compressed reference capacitor. The low-voltage arm consists of ceramic capacitors on the feedback loop of a buffer amplifier, which enables a load independent output and very small phase error in power frequency. A well-characterized Rogowski coil is used as the current sensor. The outputs of the voltage and current sensors are measured using 8½ digit sampling multimeters, which are synchronized using an external trigger generator. The developed loss measuring system was used to measure losses of an air-core reactor during 16-hour temperature rise tests according to IEC 60076-6. The test object was an air-core shunt reactor with nominal inductance of 11.7 mH. The tests were performed with 1200 A, while the feeding voltage was a few kilovolts. Results show the losses of the air-core reactor as function of time during the heating. Measured losses were also compared to the temperature compensated loss calculation, where the losses measured on cold coil are corrected to the reference steady state temperature according to IEC 60076-1.

1 INTRODUCTION

Transmission and distribution of electrical energy has losses because the high-voltage components and cables placed in the electricity grid have losses. Significant part of the losses is caused by unwanted resistance, which converts electricity to heat. In 2017, the electricity transmission losses were approximately 1.3 % and distribution losses 2.0 % of the yearly electricity consumption in Finland. Cost of these almost 2.8 TWh losses are tens of millions of euros annually for the system operators in Finland only. [1, 2].

Industry tries to manufacture grid components that have low losses but still a competitive price. Often the products are designed so that they fulfil the given energy efficiency requirements with minimum tolerance in order to avoid any over-engineering and loss of excess material keeping the product price reasonable. Low uncertainty of loss measurement is therefore important. Accurate loss measurement system will both help with the development of new low-loss products and verification of the actual losses of the final product.

Power transformers and reactors are commonly used inductive grid components with low losses. Due to the dominating inductive reactance their power factor can be very low, even 0.001, which causes challenges to the loss measurements. With

low power factor the uncertainty of the loss measurement is highly dependent on the accuracy of the measurement of the phase angle between the voltage and current. Finding and characterizing a voltage sensor with small phase uncertainty is often the most challenging part, while the phase performance of current sensors and measurement systems pose less challenges.

This study represents the loss measuring system of VTT MIKES highlighting the new voltage sensor. The performance of the measuring system is demonstrated by measuring losses of an air-core shunt reactor with very low power factor. Measurements were performed during temperature rise tests specified in IEC 60076-6 [3]. Direct loss measurements were compared to the temperature compensated loss calculation, where the losses measured on cold coil are corrected to the reference steady state temperature according to IEC 60076-1 [4].

2 LOSS MEASURING SYSTEM OF VTT MIKES

A new advanced loss measuring system was used for measuring the losses of an air-core reactor under high voltage. The system consists of a capacitive voltage divider, a current sensor and two sampling digital multimeters (DMM), which are synchronized using an external trigger generator.

Software is used to control the multimeters, to correct systematic errors of the used sensors and multimeters, and to calculate the results. Basic principle of the complete system is presented in Figure 1.

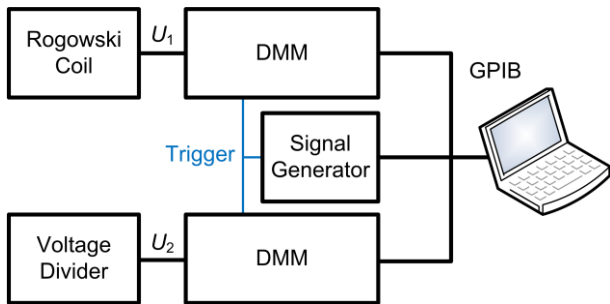


Figure 1: Basic principle of the loss measuring system. U_1 is the voltage measured from the output of the Rogowski coil and U_2 is the voltage measured from the output of the voltage divider.

2.1 Voltage divider

VTT MIKES designed and built a capacitive high-voltage divider aiming to better than $40 \mu\text{V/V}$ ratio uncertainty and $25 \mu\text{rad}$ phase displacement uncertainty. VTT MIKES approach was to use a gas-compressed reference capacitor as a high-voltage arm. The low-voltage arm presented in Figure 2 consists of ceramic capacitors on the feedback loop of a buffer amplifier, which enables a load independent output and very small phase error in power frequency. Design is similar to that described by Mohns et al. [5]. Two battery powered low-voltage arms were built with capacitance values of 290 nF and 3600 nF . They can be used with any of the high-voltage capacitors of VTT MIKES. 20 kV (100 pF) and 100 kV (37 pF) capacitors were used during the measurements presented in this paper.

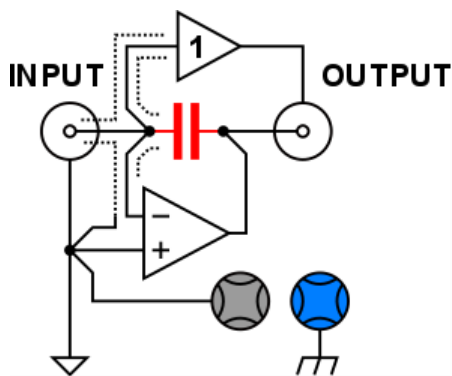


Figure 2: Main diagram of the designed low-voltage part.

The new voltage dividers were first compared to a reference measuring systems with known phase error in VTT MIKES laboratory. Comparisons were performed with low and high voltage. Low-voltage reference was a capacitive voltage divider (max.

500 V) and high-voltage reference was a 10 kV voltage transformer. After software corrections, the aimed phase displacement uncertainty ($25 \mu\text{rad}$) was achieved in the laboratory conditions. Figure 3 shows the complete 100 kV voltage divider.



Figure 3: The 100 kV capacitive voltage divider with active low voltage arm. High-voltage arm capacitance is 37 pF and low-voltage arm 290 nF .

2.2 Current sensor

Current measurement of the system is based on a Rogowski coil [6]. A well-characterized commercial Rogowski coil was used without an integrator because it allows high currents to be measured very linearly. Split core Rogowski coil was chosen because it allows easy connection to the circuit. The drawbacks related to Rogowski coils are their sensitivity to temperature [7] and conductor geometry [8]. The coil was placed in the ground side of the circuit as seen in Figure 4. After properly placed, it was calibrated in this setup against a reference zero-flux transformer. This reduces the uncertainties related to the conductor position because the circuit did not change during the measurements.



Figure 4: Rogowski coil installed in the ground side of the measurement circuit.

2.3 Meters and software

The signals from the voltage divider and the Rogowski coil were sampled using two 8½ digit sampling multimeters. DC mode of the meters were used for the sampling [9]. An external trigger generator was used to synchronize the sampling of the two multimeters with the signal.

A laptop with custom software was used to control the multimeters and the trigger generator during the measurements. Software corrects characterized systematic errors related to the analog path bandwidth and to the finite integration time of the AD converters of the meters. Calibrated phase errors of the used voltage and current sensors are also corrected for. Analysis of the data is performed in frequency domain by using Fast Fourier Transform (FFT). From several power related outputs of the software, the resistance of the test object was the main interest in this study.

3 TEMPERATURE RISE TEST FOR AN AIR-CORE SHUNT REACTOR

Loss measurements for an air-core shunt reactor were performed during temperature rise test according to IEC 60076-6. This test is performed to ensure that the temperature of the reactor stays within specification when operating voltage is applied for several hours, until thermal equilibrium has been reached [10].

Test was performed twice within one month for the same test object. Test object was an air-core shunt reactor with nominal inductance of 11.7 mH and nominal current of 1650 A. The reactor and the test setup are shown in Figure 5. In this case, the power factor was close to 0.003.

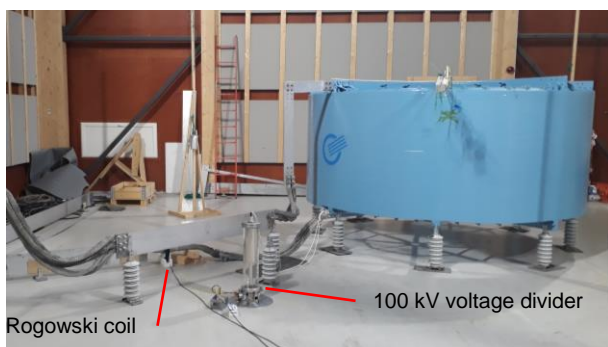


Figure 5: Blue air-core shunt reactor on the right was used as the test object during the temperature rise test.

Tests were performed in a custom test laboratory. Conducting construction materials and current loops were avoided during the construction of the laboratory to minimise their influence to the measured losses. Power was generated using

parallel resonance circuit fed by a power source with stable 50 Hz frequency.

3.1 Resistance change measured with the loss-measuring system

The presented high-voltage loss measuring system was used to measure resistance of the reactor during the temperature rise tests. During the tests 4.4 kV voltage was applied to the reactor while the current was 1200 A.

Feeding and measurement connections to the test object are presented in Figure 6. High-voltage side of the feed was connected to the upper terminal using radially connected aluminium busbar so that it would affect to the losses as low as possible. Ground return was connected to the lower terminal using thick copper braid. Braid was oriented to the same direction as the high-voltage busbar.



Figure 6: High voltage was connected to the upper terminal and ground return to the lower terminal. High-voltage measurement connection is shown as dashed white line.

High voltage divider was connected between the upper and lower terminal using white two insulated high-voltage cables shown in Figure 6. Ground side of the divider is connected directly to the lower terminal with a separate connection so that it is not part of the main current path. High-voltage side is connected to the upper terminal in similar way except the cable was positioned so that it went through the center of the reactor and then headed directly towards the lower terminal. The high-voltage and ground cables were then twisted and finally connected to the voltage divider. The 20 kV divider was used during the first temperature rise test and the 100 kV divider during the second temperature rise test.

Figures 7 and 8 show the behaviour of the resistance and current as function of time during the first and second temperature rise tests. Resistance starts to increase immediately after turning the

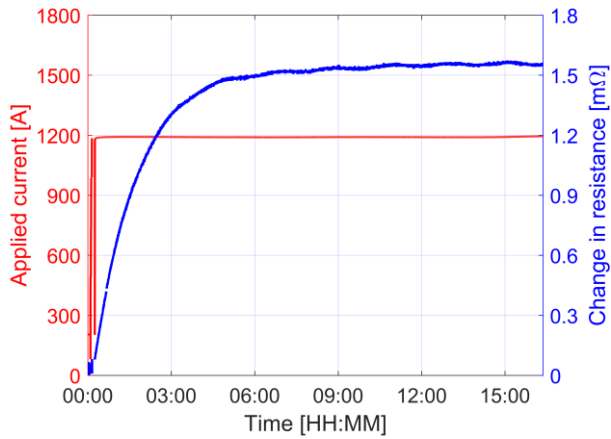


Figure 7: Measured change of resistance as function of time during the first temperature rise test. Small gaps in the beginning part of the curve are due to short breaks needed for practical arrangements.

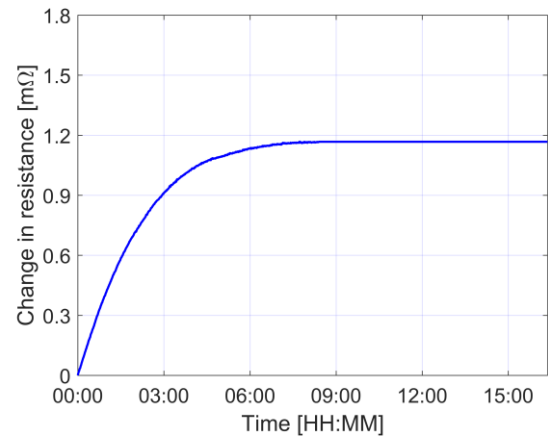


Figure 9: Calculated change of resistance as function of time during the first temperature rise test.

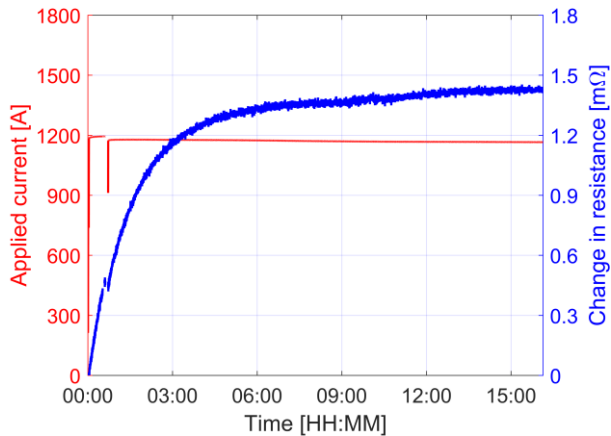


Figure 8: Measured change of resistance as function of time during the second temperature rise test. Small gaps in the beginning part of the curve are due to short breaks needed for practical arrangements.

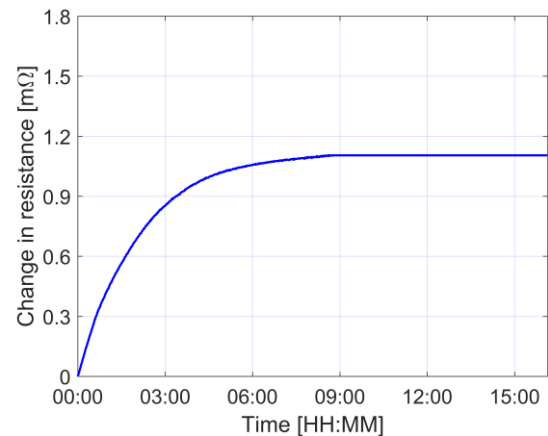


Figure 10: Calculated change of resistance as function of time during the second temperature rise test.

power on. After 8 hours temperatures and the resistance value starts to stabilize.

During the tests less than 4 % deviations were found in the absolute values of measured resistance. Systematic problem was located to the used multimeters which seem to be sensitive to external magnetic field. However, the system is expected to work very accurately when used to measure changes in stable conditions. That is why given uncertainties are lower than what would be given for absolute values.

During the first 16-hour temperature rise test the measured resistance changed 1.55 mΩ. During the second temperature rise test the change was 1.43 mΩ. Type A related uncertainties are less than 0.01 mΩ in both tests. Uncertainties related to the

measuring system are less than 0.2 mΩ. Total estimated uncertainty for the resistance change in both sessions is less than 0.2 mΩ ($k = 2$).

3.2 Resistance change according to the IEC calculation

IEC 60076-1 Annex E provides a formula for temperature correction of load-loss [4]. The average temperature rise of the reactor is needed for this calculation. The average temperature rise was determined according to IEC 60076-2 clause 7.8 [11] by measuring the DC resistance of the reactor in room temperature and then again right after the temperature rise test. The average temperature rise ΔT_{avg} can be then calculated with the following formula:

$$\Delta T_{avg} = \frac{R_{DC_hot}}{R_{DC_room}} \times (225 + T_{room}) - 225 - T_{amb_avg} \quad (1)$$

where

- R_{DC_hot} is the DC resistance measured after the temperature rise test,
- R_{DC_room} is the DC resistance measured at ambient temperature T_{room} ,
- T_{amb_avg} is the ambient temperature after the temperature rise test, and
- 225 is a constant related to aluminium properties.

Unit for temperature is degrees Celsius.

Resistance was measured with 10 A current using commercial resistance meters. Uncertainty for the R_{DC_room} is estimated to be 0.1 % ($k = 2$). Measurement of R_{DC_hot} includes practical challenges. In addition to the uncertainty of the four-terminal DC resistance measurement, also the time needed for the R_{DC} measurement after the temperature rise test affects to the result. Switching the power off, disconnecting the power source and performing the DC resistance measurement must be done quickly. The first DC resistance measurement is recommended to be performed within 2 minutes after shutdown [10]. The actual resistance at the time of shutdown was linearly extrapolated from the DC resistance data during the cooling. Total expanded uncertainty for the R_{DC_hot} is expected to be less than 0.2 % ($k = 2$).

Main uncertainty component for temperatures T_{room} and T_{amb_avg} is the standard deviation between several sensors that were located in different locations in the laboratory near the reactor. Total expanded uncertainty for these temperatures is expected to be less than 1.4 °C. By calculating the equation 1, average temperature rises were 39.6 °C and 39.3 °C during the two tests. Total expanded uncertainty ($k = 2$) for the average temperature rise is less than 2.2 °C.

Temperature of the hot top part of the reactor was measured directly with temperature sensors. Average temperature curve was created by assuming that the average and hot temperatures reach equilibrium simultaneously and long-term temperature division across the reactor stays relatively unchanged. A fourth degree polynomial was fitted to the hot temperature curve and it was scaled so that the temperature rise ends at the temperature, which was defined using the calculated average temperature rise from equation 1.

Estimated average temperature as function of time can be used to calculate the resistance change of the reactor using equation 2, which determines temperature correction for ohmic and additional

losses. Ohmic losses are increased and additional losses are decreased when temperature rises.

For aluminium reactor the resistance R_{AC_T2} at temperature T_2 can be calculated according to:

$$R_{AC_T2} = \frac{225 + T_2}{225 + T_1} \times R_{DC_T1} + \frac{225 + T_1}{225 + T_2} \times (R_{AC_T1} - R_{DC_T1}) \quad (2)$$

where

- R_{AC_T1} is the resistance measured with alternating current at temperature T_1 , and
- R_{DC_T1} is the DC resistance measured at temperature T_1 .

Unit for temperature is degrees Celsius. R_{AC_T1} was measured with an uncertainty less than 0.1 % ($k = 2$).

Calculated changes of resistance as function of time are presented in Figures 9 and 10. Waveshapes are estimations but the actual change of resistance at shutdown is according to equations 1 and 2. The change of resistance during the first temperature rise test was 1.17 mΩ. During the second temperature rise test the change was 1.10 mΩ. By

analysing the equation 2, total expanded uncertainty ($k = 2$) for the estimated resistance change is less than 0.10 mΩ.

3.3 Comparison between the results

Measured and calculated resistance change curves resemble each other well. However, the final resistance changes have a systematic difference in both temperature rise tests. Differences between the two methods were 0.38 mΩ and 0.37 mΩ so that the measured resistance change is larger than the one estimated by IEC method. Differences are larger than their estimated uncertainties. Difference was very constant in both cases even though the measurements were performed at different times and by using different voltage dividers. Current was slightly lower in the second test which can be the reason for the lower resistance changes during the test. Resistance changes are presented in Table 1.

Table 1: Resistance changes during the two temperature rise tests.

| Result | ΔR [mΩ] | Uncertainty [mΩ] |
|--------------------------|--------------------|---------------------|
| Temperature rise test 1: | | |
| Measured | 1.55 | 0.20 |
| Calculated | 1.17 | 0.10 |
| Temperature rise test 2: | | |
| Measured | 1.47 | 0.20 |
| Calculated | 1.10 | 0.10 |

4 CONCLUSIONS

An advanced loss-measuring system with its voltage divider was introduced. System can be used to measure single phase losses with low power factors up to 200 kV. With power factor of 0.001, total expanded uncertainty of 5 % ($k = 2$) for active power can be achieved. In this study, the high external magnetic field posed challenges to instrumentation, which made claiming the uncertainty of the absolute values difficult. More work has to be done for characterization and protection of the measuring setup to high external magnetic field. However, system is expected to work very accurately when used to measure changes.

Use of the measuring system was demonstrated by measuring losses of an air-core shunt reactor during temperature rise tests. Results were compared to the losses calculated according to IEC 60076-1. Calculated changes of resistance were systematically lower than the ones measured with the loss measuring system. However, they were in the same order of magnitude. One reason for differences might be that the used equations are quite simplified and expect the additional losses to decrease linearly as function of temperature.

ACKNOWLEDGMENTS

The work reported here has received support from the EMPIR programme co-financed by the Participating States and from the *European Union's Horizon 2020 research and innovation programme*.

Authors would like to thank laboratory manager Pekka Nevalainen and his colleague Jyrki Väätäinen from the support during the on-site measurements.

REFERENCES

- [1] Finnish Energy. Electricity balance 1970-2017, published 27.9.2018. URL: https://energia.fi/en/news_and_publications/publications/electricity_balance_1970-2017.html, last accessed January 10, 2019.
- [2] Nordpool. Elspot prices 2017. URL: <https://www.nordpoolgroup.com/historical-market-data/>, last accessed January 10, 2019.
- [3] IEC 60076-6.Ed.1.0, "Power transformers - Part 6: Reactors", 2007.
- [4] IEC 60076-1.Ed.3.0, "Power transformers - Part 1: General", 2011.
- [5] E. Mohns, J. Chunyang, H. Badura and P. Raether, "An Active Low-Voltage Capacitor for Capacitive HV Dividers," *2018 Conference on Precision Electromagnetic Measurements (CPEM 2018)*, Paris, 2018, pp. 1-2. doi: 10.1109/CPEM.2018.8501238
- [6] A. P. Chattock: "On a Magnetic Potentiometer",

Philosophical Magazine and Journal of Science, vol. XXIV, no. 5th Series, pp. 94–96, 1887.

- [7] J. Hällström, E.-P. Suomalainen: "Rogowski Coil Setup for Calibration of AC Currents up to 10 kA", *CPEM 2006 Conf. Digest*, Torino, Italy, pp. 210-211, 2006.
- [8] E.-P. Suomalainen, J. Hällström: "Onsite Calibration of a Current Transformer Using a Rogowski Coil", *IEEE Trans. Instrum. Meas.*58, pp.1054–1058, 2009.
- [9] R. Lapuh: "Sampling with 3458A". Left Right d.o.o. ISBN 978-961-94476-0-4 1st edition, 2018.
- [10] IEC 60076-11.Ed.2.0, "Power transformers - Part 2: Dry-type transformers", 2018.
- [11] IEC 60076-6.Ed.3.0, "Power transformers - Part 2: Temperature rise for liquid-immersed transformers", 2011.